American Mineralogist, Volume 102, pages 1771–1775, 2017

ACTINIDES IN GEOLOGY, ENERGY, AND THE ENVIRONMENT

Crystal structure of richetite revisited: Crystallographic evidence for the presence of pentavalent uranium

Jakub Plášil[1,*]

[1]Institute of Physics ASCR, v.v.i., Na Slovance 2, CZ–182 21, Praha 8, Czech Republic

Abstract

Revision of crystal structure of the rare U-oxide mineral richetite provided crystallographic evidence for the presence of pentavalent U. The structure of richetite, space group $P\bar{1}$, a = 12.0919(2), b = 16.3364(4), c = 20.2881(4) Å, α = 68.800(2), β = 78.679(2), γ = 76.118(2)°, with V = 3600.65(14) Å^3 and Z = 1, was solved by charge-flipping algorithm and refined to an agreement index (R) of 5.6% for 9955 unique reflections collected using microfocus X-ray source. The refined structure, in line with the previous structure determination, contains U-O-OH sheets of the α-U_3O_8 type (protasite topology) and an interstitial complex comprising Pb^{2+}, Fe^{2+}, Mg^{2+} cations and molecular H_2O. However, the polyhedral geometry, the bond-valence sum incident at one U site within the sheet (U17) together with charge-balance requirements, indicate that U17 site is occupied by U^{5+}. The U17Φ_7 (Φ: O, OH) polyhedra is distorted, with two shorter U–O bond-lengths (~2.01 Å), four longer U–O bond-lengths (~2.2 Å) and one, very long U–O bond (2.9 Å). The color of richetite also supports the presence of U^{5+} in the structure The current results show that α-U_3O_8 type of sheet can incorporate U^{5+}. Richetite is the third mineral containing pentavalent uranium that occurs in nature.

Keywords: Richetite, uranyl oxide hydroxy-hydrate, crystal structure, pentavalent uranium, weathering

Introduction

Uranyl-oxide hydroxy-hydrate minerals (further labeled as UOH) are important products of supergene weathering of primary U^{4+} minerals, predominantly uraninite. They form in the initial alteration stages and are common constituents of the oxidized parts of uranium deposits, and usually replace uraninite in situ, forming massive aggregates called "*gummites*" (Finch and Ewing 1992; Finch and Murakami 1999; Krivovichev and Plášil 2013; Plášil 2014). Weathering of uraninite, also called hydration-oxidation weathering, is of further relevance because of the analogy between the alteration of uraninite and UO_{2+x} in spent nuclear fuel (Janeczek et al. 1996). The crystallography and crystal chemistry of this mineral group has attracted a lot of attention and this group is nowadays extensive (see e.g., Plášil et al. 2016). These minerals and the synthetic UOH phases have been studied intensively by X-ray diffraction and only a few of their structures are unknown.

Richetite is a rare UOH mineral, occurring at few localities in the world. It was originally described by Vaes (1947) from Shinkolobwe mine, Haut-Katanga province, Democratic Republic of Congo, Africa, and later studied by Piret and Deliens (1984). Richetite has a large triclinic unit cell (Burns 1998), which is in line with results of Piret and Deliens (1984). However, the structure has several issues prompting reexamination of the structure.

Redetermination of the crystal structure

The crystal used in this study was obtained from a sample provided by Jean-Claude Leydet (Brest, France) and originates from the type locality, Shinkolobwe mine (Haut-Katanga province, DRC, Africa).

A tabular grayish brown fragment of richetite was selected under an optical microscope and used for X-ray study. Data were collected using a Rigaku (Oxford diffraction) SuperNova diffractometer, using Mo$K\alpha$ radiation (λ = 0.71073 Å) from a micro-focus X-ray tube collimated and monochromatized by mirror optics and detected by an Atlas S2 CCD detector. From 39 599 collected reflections, 13 469 were independent and 9955 were unique observed with the criterion $I_{obs} > 3\sigma(I)$. Integration of the diffraction data, including corrections for background, polarization and Lorentz effects, was done using the CrysAlis RED program. The absorption correction combining empirical scaling and spherical-absorption correction was done with CrysAlis program; SCALE3 Abspack algorithm.

The structure of richetite was solved by the charge-flipping algorithm using the SHELXT program (Sheldrick 2015). The structure model was refined by full-matrix least-squares in the Jana2006 program (Petříček et al. 2014) based on F^2. The reflection conditions were consistent with the space-group $P\bar{1}$, which was further confirmed by the successful refinement. The possibility for twinning by reticular merohedry was tested by Jana2006 (Petříček et al. 2016) (transformation matrix 1 –2 –1/1 0 0/0 –1 1), however it was negative. The crystal used for the experiment was found to be a split crystal; the contribution of the second fragment to the data set was corrected by detecting

* E-mail: Plasil@fzu.cz

Special collection papers can be found online at http://www.minsocam.org/MSA/AmMin/special-collections.html.

0003-004X/17/0009–1771$05.00/DOI: http://dx.doi.org/10.2138/am-2017-6092

fully separated, fully overlapped and partially separated reflections in Jana2006 (Petříček et al. 2016). The structure solution provided nearly complete structure sheets and missing atoms (mostly O atoms) were located from the difference-Fourier maps. Anisotropic displacement parameters were used for U, Pb, and Fe atoms. Unconstrained and unrestrained refinement converged smoothly to final $R = 0.056$ for 9955 unique observed reflections (Table 1). Final atom coordinates and displacement parameters are listed in Supplemental[1] Tables 1 and 2, selected interatomic distances are in Supplemental[1] Tables 3 and 4, and the bond-valence sums (calculated by the procedure of Brown 1981, 2002) are listed in Supplemental[1] Table 2. The original crystallographic information file (cif) is provided with the supplementary material[1].

Description of the crystal structure

The structure of richetite contains 18 unique U sites, 8 unique Pb sites, 1 mixed Fe/Mg site, and 85 O sites (of which 18 correspond to H_2O groups) (Fig. 1). The U sites are coordinated by seven ligands (O or OH^-) in two classes of distances: ~1.8 Å and 2.1 to ~2.8 Å. as it is characteristic for the UO_2^{2+} ion (Evans 1963; Burns et al. 1997a; Lussier et al. 2016). The structure contains 8 Pb sites; none of them is fully occupied, site-scattering refinement showed occupancies ranging from 0.14 to 0.95. The coordination polyhedra around Pb atoms are irregular; ligands are represented by O_{Ur} atoms and H_2O groups, with Pb–Φ bond

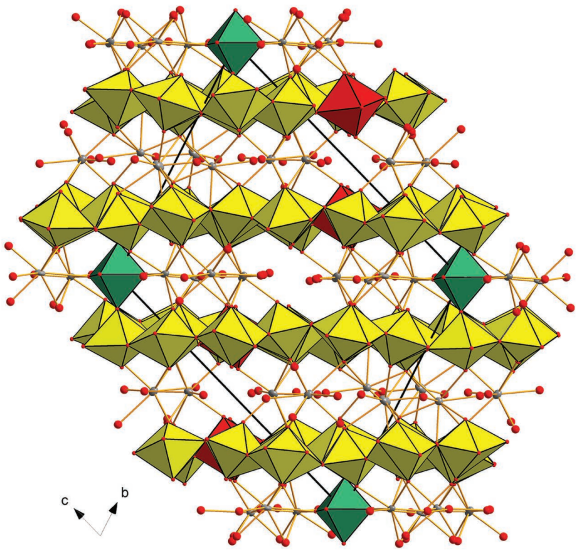

Figure 1. Crystal structure of richetite viewed down **a**. Uranyl polyhedra are drawn in yellow color, except of $U^{5+}17$ polyhedra (red); M^{2+} octahedra are green, Pb atom dark gray, and O atoms are displayed as red balls. Unit-cell edges are outlined in solid black line. (Color online.)

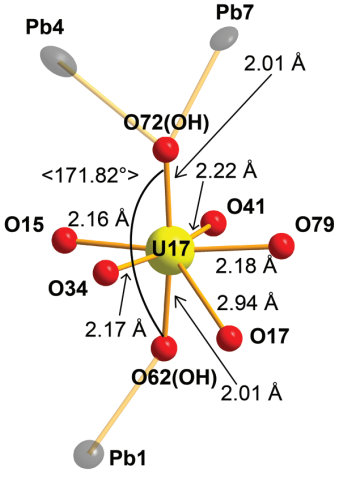

► **Figure 2.** Coordination environment around U17 site, occupied by U^{5+}, with displayed bond lengths and O–U–O bonding angle. (Color online.)

lengths ranging from 2.4 to 3.1 Å (Table 2). Richetite structure contains also one symmetrically unique octahedrally coordinated site, occupied by divalent cations Fe^{2+} and Mg^{2+}, with $<M^{2+}–Φ>$ bond-length of 2.07 Å. The M^{2+} octahedron is quite regular and is formed by two O_{Ur} atoms (of the U2) and four H_2O groups. Site-scattering refinement gave $M^{2+} = 0.62\ Fe^{2+} + 0.38\ Mg^{2+}$.

The U17 site

Several U sites in the structure of richetite exhibit irregular coordination. In case of U17 (Fig. 2; Supplemental[1] Table 4) O62 and O72 atoms (OH groups), which usually should be O_{Ur} atoms with U–O bond-lengths of 1.8 Å, have U–O distances of 2.006(19) and 2.01(2) Å. Moreover, O62–U17–O72 bond-angle is 171.82°, different from the usually linear UO_2^{2+} ion. Bond-valence analysis (Supplemental[1] Table 2) indicates that the U17 site is occupied by pentavalent U.

[1]Deposit item AM-17-96092, Supplemental Tables and cif. Deposit items are free to all readers and found on the MSA web site, via the specific issue's Table of Contents (go to http://www.minsocam.org/msa/ammin/toc/2017/Sep2017_data/Sep2017_data.html).

Table 1. Summary of data collection conditions and refinement parameters for richetite

Structural formula	$(Fe^{2+}_{0.31}Mg_{0.19})Pb_{4.86}[U^{5+}(U^{6+}O_2)_{17}O_{18}(OH)_{14}](H_2O)_{\sim 19.5}$
Unit-cell parameters	$a = 12.0919(2)$, $b = 16.3364(4)$, $c = 20.2881(4)$ Å $\alpha = 68.800(2)$, $\beta = 78.6794(18)$, $\gamma = 76.1181(19)°$
V	3600.68(14) Å^3
Z	2
Space group	$P\bar{1}$
D_{calc} (g/cm^3)	6.194 (for the formula given above)
Temperature	298 K
Diffractometer	Rigaku SuperNova, Atlas S2 CCD
Radiation (wavelength)	Mo$K\alpha$ (0.7107 Å)
Crystal dimensions	0.174 × 0.135 × 0.029 mm
Collection mode	ω scans to cover the Ewald sphere
Frame width, counting time	1.0°, 300 s
Limiting θ angles	3.40–28.10°
Limiting Miller indices	$-15 < h < 15$, $-21 < k < 21$, $-26 < l < 26$
No. of reflections	39599
No. of unique reflections	13469
No. of observed reflections (criterion)	9955 $[I_{obs} > 3\sigma(I)]$
μ (mm^{-1})	51.76
T_{min}/T_{max}	0.055/0.079
Coverage, R_{int}	0.98, 0.043
F_{000}	5479
Refinement	Full matrix least-squares by Jana2006 on F^2
Parameters refined	593
R, wR (obs)	0.0560, 0.1142
R, wR (all)	0.0771, 0.1210
GOF (obs, all)	1.99, 1.80
Weighting scheme	$1/(\sigma 2(I) + 0.0004I2)$
$\Delta\rho_{min}$, $\Delta\rho_{max}$ (e/Å^3)	−4.12, 6.56 (1.29 Å from O70 atom)
Twin ratio; twin matrix	0.8482(17)/0.15118(17); $\begin{pmatrix} -1 & 0 & 0 \\ 0 & -0.328 & -0.671 \\ 0 & -1.328 & 0.328 \end{pmatrix}$

TABLE 2. Comparison of the U17Φ_7 polyhedral geometry in richetite with other compounds

	U–Φ (Å)							O–U–O (°)	BV (v.u.)	Ref.
Richetite (U17)	2.161	2.943	2.166	2.228	2.01	2.01	2.186	171.8	5.37	this work
Wyartite (U3)	2.07	2.09	2.06	2.14	2.44	2.47	2.480	167.0	5.07	1
Dehyd. wyartite (U2)	2.095	2.095	2.092	2.092	2.476	2.512	2.301	163.6	5.10	2
U_2MoO_8	2.06	2.06	2.11	2.18	2.36	2.46	2.73	178.1	4.92	3
	2.08	2.08	2.13	2.15	2.32	2.35	2.58	164.1	5.12	
$USbO_5$	1.93	2.02	2.13	2.30	2.35	2.43	2.50	173.0	5.23	4
UVO_5	2.05	2.07	2.21	2.21	2.30	2.30	2.32	179.9	5.26	5
$U_5O_{12}Cl$	2.06	2.06	2.25	2.25	2.30	2.30	2.54	178.9	4.95	6

Note: 1 = Burns and Finch (1999); 2 = Hawthorne et al. (2006); 3 = Serezhkin et al. (1973); 4 = Dickens and Stuttard (1992); 5 = Dickens et al. (1992); 6 = Cordfunke et al. (1985).

The sheets of polyhedra

The sheet of polyhedra found in richetite has the protasite uranyl–anion topology, i.e., the α-U_3O_8 sheet (Fig. 3) (Burns 1998, 2005; Lussier et al. 2016). All pentagons are occupied by U atoms, the U17 site by U^{5+}, and the rest by U^{6+}. Based upon distribution of $(OH)^-$ within the equatorial ligands (excluding two OH groups associated with U17), we can distinguish several structures of protasite topology. In richetite (Burns 1998), we have the AABAAB... sequence, where considering type-A triangles [which have (OH) groups at all corners], and type-B triangles (which contain only O^{2-} anions), richetite has twice as many A triangles as B triangles. The O:OH ratio in richetite is 3:2, however, there are also two OH groups linked to U17 (in case of other U sites in richetite, they are O_{Ur} atoms), linking U17 to Pb1 through O62, and to Pb4 and Pb7 through O72. In case of protasite (Pagoaga et al. 1987), all (OH) groups are located at the corners of triangles of the topology, such that all triangles in the sheet contain two (OH) groups. The sheets in the structures of becquerelite (Burns and Li 2002) and billietite (Finch et al. 2006) (considering there the α-U_3O_8 sheet only) have the composition $[(UO_2)_6O_4(OH)_6]^{2-}$ with O:OH = 2:3. In the becquerelite and billietite sheet anion-topologies, all (OH) groups are located at the corners of triangles, and all triangles contain three (OH) groups.

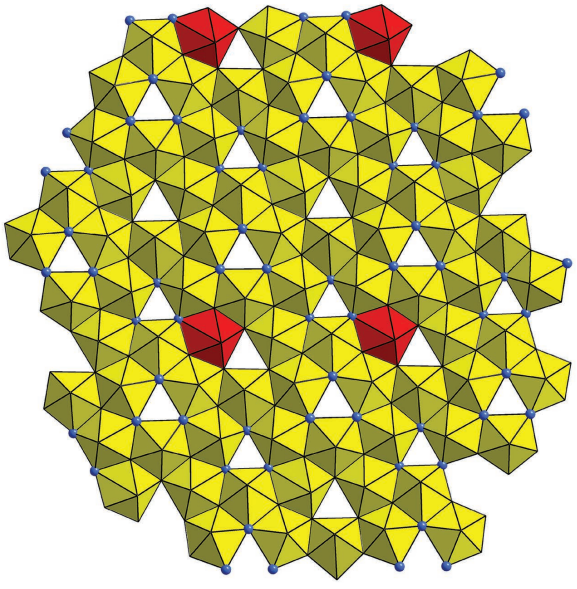

FIGURE 3. Sheet of uranyl polyhedra of the α-U_3O_8 type (or protasite topology) found in the structure of richetite. In red is displayed U17 polyhedron, occupied by U^{5+}; the distribution of OH groups within the sheet is shown by blue balls. (Color online.)

The interlayer complex

As indicated by Burns (1998), the structure of richetite contains two different interlayer complexes containing Pb^{2+}, M^{2+} and H_2O groups. Adjacent sheets of protasite topology are linked through an extensive network of Pb–O, M^{2+}–O, and O–H···O bonds. The interstitial complex comprising M^{2+} octahedra occurs at **b** = 0, **c** = 0, and is built from two tetramers (Pb2, Pb4, Pb7, and Pb8) linked by M^{2+} octahedra (Fig. 4). Four of the ligands coordinated to M^{2+} site are H_2O groups, and two are O_{Ur} atoms. There is an additional O site (O84) that is occupied by an H_2O group that links to the structure through H-bonds only. The coordination environment of the corresponding Pb sites is shown in Figure 4.

The interlayer complex that does not contain the M^{2+} site occurs at **b** ~0.5, **c** ~0.5. It contains a dimer of Pb1Φ_8 and Pb3Φ_9 (Φ = O, OH, H_2O) polyhedra and a tetramer of Pb5Φ_8 and Pb6Φ_8 (Φ = O, H_2O) polyhedra (Fig. 5). Between these clusters of polyhedra there are three independent O sites that belong to H_2O groups that are not coordinated directly to any metal cation site.

The structural formula

The structural formula of the studied richetite crystal is therefore $M^{2+}_{0.50}Pb_{4.86}[U^{5+}(U^{6+}O_2)_{17}O_{18}(OH)_{14}](H_2O)_{\sim 19.5}$, $Z = 2$. This formula is in line with the color of richetite (Fig. 6). Most UOH minerals are orange or yellow, whereas those minerals containing U^{5+}, wyartite (Burns and Finch 1999) and dehydrated wyartite (Hawthorne et al. 2006) are similar in color to richetite.

α-U_3O_8 topology and the presence of U^{5+}

Incorporation of U^{5+} into α-U_3O_8 type sheets has not been considered; all minerals with U^{5+} or U^{4+} present adopt β-U_3O_8 sheets (Burns and Finch 1999; Burns et al. 1997b; Hawthorne et al. 2006). For shinkolobweite, $Pb_{1.25}[U^{5+}(H_2O)_2(UO_2)_5O_8(OH)_2](H_2O)_5$ (Olds et al. 2017), there are sheets resembling β-U_3O_8 topology. Geometrically, the U17 site in richetite is consonant with the idealized α-U_3O_8 topology and bond-valence analysis clearly indicates incorporation of U^{5+}. Thus, incorporation of U^{5+} into α-U_3O_8 topology is possible.

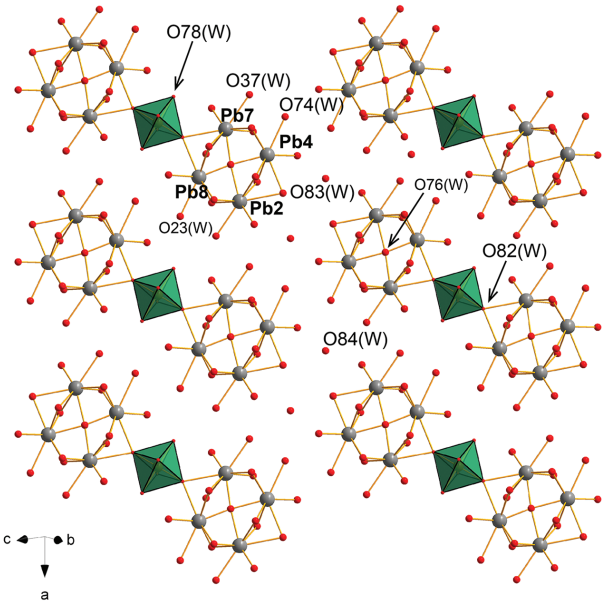

FIGURE 4. Interstitial constituents at **b** ~0, **c** ~0 (extended to for about four unit-cell content). The M^{2+} (mixed Fe1/Mg1 site) octahedra are shown in green color, Pb^{2+} sites are dark gray, O atoms are represented by red balls. H_2O groups are labeled (W). (Color online.)

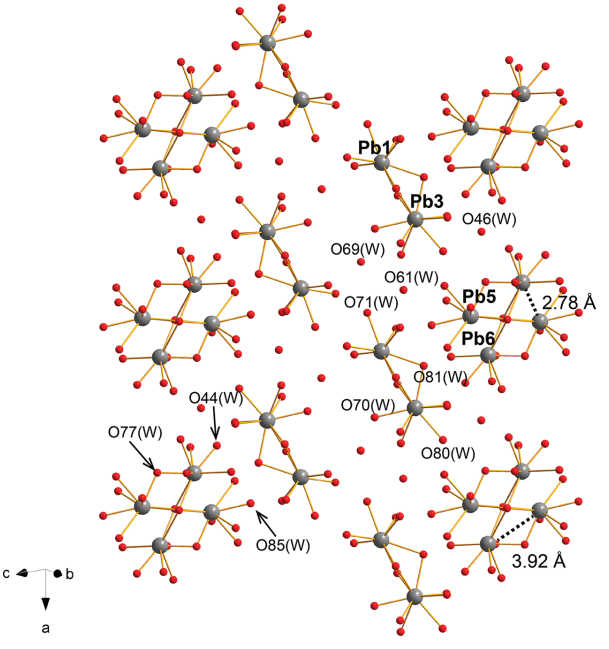

FIGURE 5. Interstitial constituents at **b** ~0.5, **c** ~0.5 (extended to for about four unit-cell content). Pb^{2+} sites are dark gray, O atoms are represented by red balls. H_2O groups are labeled (W). (Color online.)

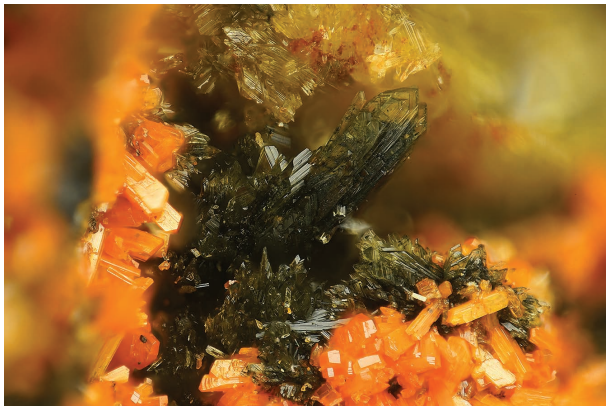

FIGURE 6. Richetite crystals (olive brown) among masuyite (orange). Shinkolobwe mine (type locality), Haute-Katanga province, DRC, Africa. FOV 2 mm, photo S. Wolfsried. (Color online.)

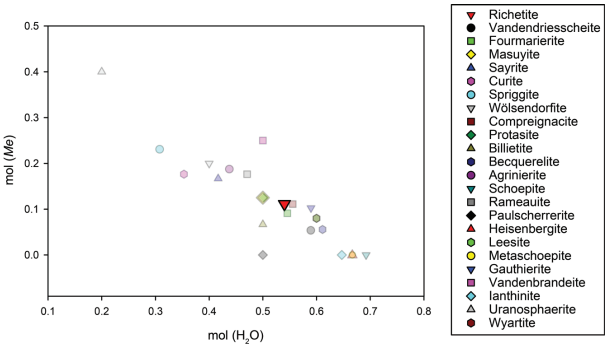

FIGURE 7. Composition of uranyl-oxide hydroxy-hydrate minerals as a function of proportion of molecular H_2O and a content of metal cations (*Me*). (Color online.)

IMPLICATIONS

UOH minerals are important products of oxidation-hydration weathering of uraninite, or UO_2 in spent nuclear fuel (Finch and Ewing 1992; Janeczek et al. 1996; Wronkiewicz et al. 1992, 1996; Krivovichev and Plášil 2013; Plášil 2014). Based on field as well as laboratory observations (for references, see above cited papers), a weathering sequence for UOH has been established (after Finch and Ewing 1992; Fig. 7). At very early stages of uraninite alteration under oxidizing conditions, result in minerals with a high-proportion of molecular H_2O and low content of metal cations such as schoepite, $[(UO_2)_8O_2(OH)_{12}](H_2O)_{12}$ (Finch et al. 1996, 1998). With increasing time UOH structures will incorporate metal cations released from the gradually weathering uraninite (such as radiogenic Pb and others) or from host-rocks (Na, K, Ca, etc.). The position of richetite in the alteration sequence is determined by the molar proportion of H_2O and *Me* close to fourmarierite, masuyite and protasite. Also the value of charge deficiency per anion (CDA; defined by Schindler and Hawthorne 2008), ~0.21 v.u., is close to that of fourmarierite (0.19 v.u.) and masuyite (0.22 v.u.). It has been shown that the CDA value correlates closely with increase of *Me* and decrease of H_2O in the structures, therefore higher CDA corresponds to older products during the weathering

sequence. There are two or three other UOH minerals that contain reduced forms of U. They are ianthinite (with U^{4+}), wyartite, and dehydrated wyartite (with U^{5+} in addition to U^{6+}). The presence of the reduced form of an easily oxidized species indicates high gradients of redox conditions within the systems where these phases form. All of these phases form during initial stages of uraninite weathering. Ianthinite is related to the schoepite family of minerals (Fig. 7); there is a solid-state spontaneous phase transition from ianthinite to schoepite. The position of wyartite is not clear; the usual mineral association comprises uranophane, schoepite and fourmarierite. Samples of ianthinite, besides those from Shinkolobwe, also come from the well-known uranium deposit Menzenschwand (Krunkelbachtal, Baden-Württemberg, Germany), where ianthinite is usually associated with pyrite and often fills vugs in altered uraninite-pyrite aggregates in a quartz matrix. Richetite forms during later stages of uraninite weathering. The presence of Fe^{2+} in richetite also indicates special geochemical conditions. It seems likely that most of sulfides (as a source of Fe) had undergone complete dissolution prior to the formation of richetite. It is clear that partial reduction of U^{6+} to U^{5+} is most probably connected to the Fe^{2+}/Fe^{3+} pair, which is also the most frequent redox agent in nature. To assess the role of Fe in the formation of richetite, more detailed textural work is needed. To conclude, minerals where U is present in a reduced valence state, such as in ianthinite, wyartite, and richetite, may play an important role during the alteration of uraninite or SNF under less-oxidizing conditions, or at places with reduced f_{O_2} or where the redox conditions are characterized by high gradients, as in roll-front, environments with extremely low pH, etc. Such phases also might play role during long-term storage of SNF in geological repositories under reducing conditions (Ewing 2015; Ewing et al. 2016).

Acknowledgments

Jean-Claude Leydet (Brest, France) is thanked for providing me a sample for single-crystal study. My thanks go to Jiří Čejka (Roudnice nad Labem, Czech Republic) for his encouragement for the study and critical reading of the manuscript and to Stephan Wolfsried (Waiblingen, Germany) for beautiful microphotography or richetite crystals. The manuscript benefited from the comprehensive thorough reviews of Sergey Krivovichev and an anonymous referee. The editorial handling of Peter Burns is highly acknowledged. This research was financially supported the Project No. LO1603 under the Ministry of Education, Youth and Sports National sustainability program I of Czech Republic.

References cited

Brown, I.D. (1981) The bond-valence method: an empirical approach to chemical structure and bonding. In M. O'Keeffe and A. Navrotsky, Eds., Structure and Bonding in Crystals II. Academic Press, New York, 1–30.

——— (2002) The Chemical Bond in Inorganic Chemistry: The Bond Valence Model. Oxford University Press, UK.

Brown, I.D. and Altermatt, D. (1985) Bond-valence parameters obtained from a systematic analysis of the inorganic crystal structure database. Acta Crystallographica, B41, 244-247, with updated parameters from http://www.ccp14.ac.uk/ccp/web-mirrors/i_d_brown/.

Burns, P.C. (1998) The structure of richetite, a rare lead uranyl oxide hydrate. Canadian Mineralogist, 36, 187–199.

——— (2005) U^{6+} minerals and inorganic compounds: insights into an expanded structural hierarchy of crystal structures. Canadian Mineralogist, 43, 1839–1894.

Burns, P.C., and Finch, R.J. (1999) Wyartite: crystallographic evidence for the first pentavalent-uranium mineral. American Mineralogist, 84, 1456–1460.

Burns, P.C., and Li, Y. (2002) The structures of becquerelite and Sr-exchanged becquerelite. American Mineralogist, 87, 550–557.

Burns, P.C., Ewing, R.C., and Hawthorne, F.C. (1997a) The crystal chemistry of hexavalent uranium: polyhedron geometries, bond-valence parameters, and polymerization of polyhedra. Canadian Mineralogist, 35, 1551–1570.

Burns, P.C., Finch, R.J., Hawthorne, F.C., Miller, M.L., and Ewing, R.C. (1997b) The crystal structure of ianthinite, $[U_2^{4+}(UO_2)_4O_6(OH)_4(H_2O)_4](H_2O)_5$: a possible phase for Pu^{4+} incorporation during the oxidation of spent nuclear fuel. Journal of Nuclear Materials, 249, 199–206.

Cordfunke, E.H.P., Van Vlaanderen, P.V., Goubitz, K., and Loopstra, B.O. (1985) Pentauranium(V) chloride dodecaoxide $U_5O_{12}Cl$. Journal of Solid State Chemistry, 56, 166–170.

Dickens, P.G., and Stuttard, G.P. (1992) Structure of uranium antimony oxide ($USbO_5$) powder neutron diffraction study. Journal of Materials Chemistry, 2, 691–694.

Dickens, P.G., Stuttard, G.P., Ball, R.G.J., Powell, A.V., Hull, S., and Patat, S. (1992) Powder neutron diffraction study of the mixed uranium vanadium oxides $Cs_2(UO_2)_2(V_2O_8)$ and UVO_5. Journal of Materials Chemistry, 2, 161–166.

Evans, H.T., Jr. (1963) Uranyl ion coordination. Science, 141, 154–157.

Ewing, R.C. (2015) Long-term storage of spent nuclear fuel. Nature Materials, 14, 252–257.

Ewing, R.C., Whittlestone, L.A., and Yardley, B.W.D. (2016) Geological disposal of nuclear waste: A primer. Elements, 12, 233–237.

Finch, R.J., and Ewing, R.C. (1992) The corrosion of uraninite under oxidizing conditions. Journal of Nuclear Materials, 190, 133–156.

Finch, R.J., and Murakami, T. (1999) Systematics and paragenesis of uranium minerals. In P.C. Burns and R.C. Ewing, Eds., Uranium: Mineralogy, Geochemistry and the Environment. Mineralogical Society of America and Geochemical Society. Reviews in Mineralogy and Geochemistry, 38, 91–179.

Finch, R.J., Cooper, M.A., Hawthorne, F.C., and Ewing, R.C. (1996) The crystal structure of schoepite, $[(UO_2)_8O_2(OH)_{12}](H_2O)_{12}$. Canadian Mineralogist, 34, 1071–1088.

Finch, R.J., Hawthorne, F.C., and Ewing, R.C. (1998) Structural relations among schoepite, metaschoepite and "dehydrated schoepite". Canadian Mineralogist, 36, 831–845.

Finch, R.J., Burns, P.C., Hawthorne, F.C., and Ewing, R.C. (2006) Refinement of the crystal structure of billietite $Ba[(UO_2)_6O_4(OH)_6](H_2O)_8$. Canadian Mineralogist, 44, 1197–1205.

Hawthorne, F.C., Finch, R.J., and Ewing, R.C. (2006) The crystal structure of dehydrated wyartite, $Ca(CO_3)(U^{5+}(U^{6+}O_2)_2O_4(OH))(H_2O)_3$. Canadian Mineralogist, 44, 1379–1385.

Janeczek, J., Ewing, R.C., Oversby, V.M., and Werme, L.O. (1996) Uraninite and UO_2 in spent nuclear fuel: a comparison. Journal of Nuclear Materials, 238, 121–130.

Krivovichev, S.V., and Plášil, J. (2013) Mineralogy and crystallography of uranium. in "Uranium, from cradle to grave". In P.C. Burns and G.E. Sigmon, Eds., MAC Short Course, 43, pp. 15–119, Winnipeg MB, May 2013.

Lussier, A.J., Lopez, R.A.K., and Burns, P.C. (2016) A revised and expanded structure hierarchy of natural and synthetic hexavalent uranium compounds. Canadian Mineralogist, 54, 177–283.

Olds, T.A., Lussier, A.J., Oliver, A.G., Petříček, V., Plášil, J., Kampf, A.R., Burns, P.C., Dembowski, M., Carlson, S.M., and Steele, I.M. (2017) Shinkolobweite, IMA2016-095. CNMNC Newsletter No. 36, April 2017, page 404; Mineralogical Magazine, 81, 403–409.

Pagoaga, M.K., Appleman, D.E., and Stewart, J.M. (1987) Crystal structures and crystal chemistry of the uranyl oxide hydrates becquerelite, billietite, and protasite. American Mineralogist, 72, 1230–1238.

Petříček, V., Dušek, M., and Palatinus, L. (2014) Crystallographic Computing System JANA2006: General features. Zeitschrift für Kristallographie, 229, 345–352.

Petříček, V., Dušek, M., and Plášil, J. (2016) Crystallographic computing system Jana2006: Solution and refinement of twinned structures. Zeitschrift für Kristallographie, 231, 583–599.

Piret, P. and Deliens, M. (1984) Nouvelles données sur la richetite $PbO.4UO_3.4H_2O$. Bulletin de Minéralogie, 107, 581–585.

Plášil, J. (2014) Oxidation–hydration weathering of uraninite: the current state-of-knowledge. Journal of Geosciences, 59, 99–114.

Plášil, J., Škoda, R., Čejka, J., Bourgoin, V., and Boulliard, J.-C. (2016) Crystal structure of the uranyl-oxide mineral rameauite. European Journal of Mineralogy, 28, 959–967.

Schindler, M., and Hawthorne, F.C. (2008) The stereochemistry and chemical composition of interstitial complexes in uranyl-oxysalt minerals. Canadian Mineralogist, 46, 467–501.

Serezhkin, V.N., Kovba, L.M., and Trunov, V.K. (1973) Crystal structure of U_2MoO_8. Kristallografiya, 18, 514–517 (in Russian).

Sheldrick, G.M. (2015) SHELXT—Integrated space-group and crystal-structure determination. Acta Crystallographica, A71, 3–8.

Vaes, J.F. (1947) Six nouveaux minéraux d'urane provenant de Shinkolobwe (Katanga). Annales de la Société géologique de Belgique, 70:212–225.

Wronkiewicz, D.J., Bates, J.K., Gerding, T.J., and Veleckis, E. (1992) Uranium release and secondary phase formation during unsaturated testing of UO_2 at 90°C. Journal of Nuclear Materials, 190, 107–127.

Wronkiewicz, D.J., Bates, J.K., Wolf, S.F., and Bick, E.C. (1996) Ten year results from unsaturated drip tests with UO_2 at 90°C: implications for the corrosion of spent nuclear fuel. Journal of Nuclear Materials, 238, 78–95.

Manuscript received January 31, 2017
Manuscript accepted May 4, 2017
Manuscript handled by Peter C. Burns